

LIMITS ON COMPACT HALO OBJECTS AS DARK MATTER FROM GRAVITATIONAL MICROLENSING

Philippe Jetzer

Institute of Theoretical Physics
University of Zürich

ICPF 2012, Kolymbari, Crete, Greece
June 2012

Since the discovery of the first microlensing events in 1993
More than 5000 events have been discovered:

LMC ~ 15-20 events (MACHO+EROS+OGLE)

SMC ~ 6 events (MACHO+EROS+OGLE): analysis in progress
(optical depth $\tau = 1.30 \pm 1.01 \times 10^{-7}$ based on 3 OGLE events)

Galactic Bulge region more than 4000 events!
(by MACHO, EROS, OGLE and MOA: some 10 planets!)

Spiral arms ~ 30 events

M31 ~ 35 events (by several collaborations)

Globular clusters ~ few

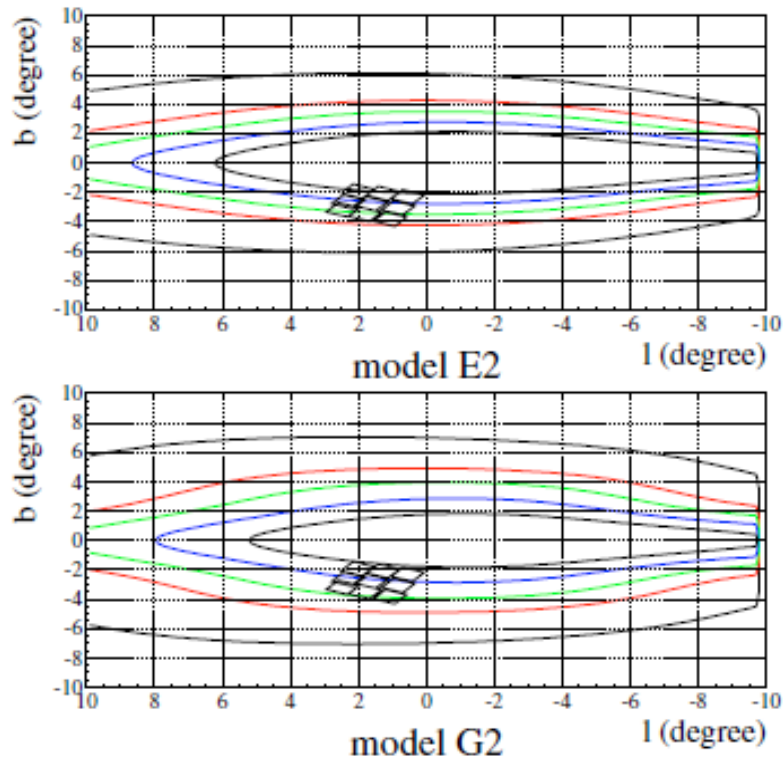


Fig. 1. Optical depth profiles as a function of the Galactic coordinates l, b for the bulge models E2 (top) and G2. The contours of the 9 MACHO CGR fields are shown. The optical depth is normalised to the value of the observed τ at position $l, b = 1^{\circ}50, -2^{\circ}68$ (see text for details). The profiles are drawn at values of $\tau = (0.3, 1.0, 1.5, 2.17, 3.0) \times 10^{-6}$. Overall, the 94 MACHO fields (Popowski et al. 2005) extend in the ranges $0^{\circ}, 8^{\circ}$ and $-2^{\circ}, -10^{\circ}$ in Galactic longitude and latitude respectively. The 66 EROS fields (Hamadache et al. 2006) cover two regions at both positive and negative Galactic latitude, $l \sim (8^{\circ}, -6^{\circ})$, $b \sim (-2^{\circ}, -6^{\circ})$ and $l \sim (6^{\circ}, -4^{\circ})$, $b \sim (2^{\circ}, 6^{\circ})$. The 30 OGLE fields analysed in Sumi et al. (2006) cover a smaller region near the Galactic centre spreading only slightly beyond the MACHO CGR fields.

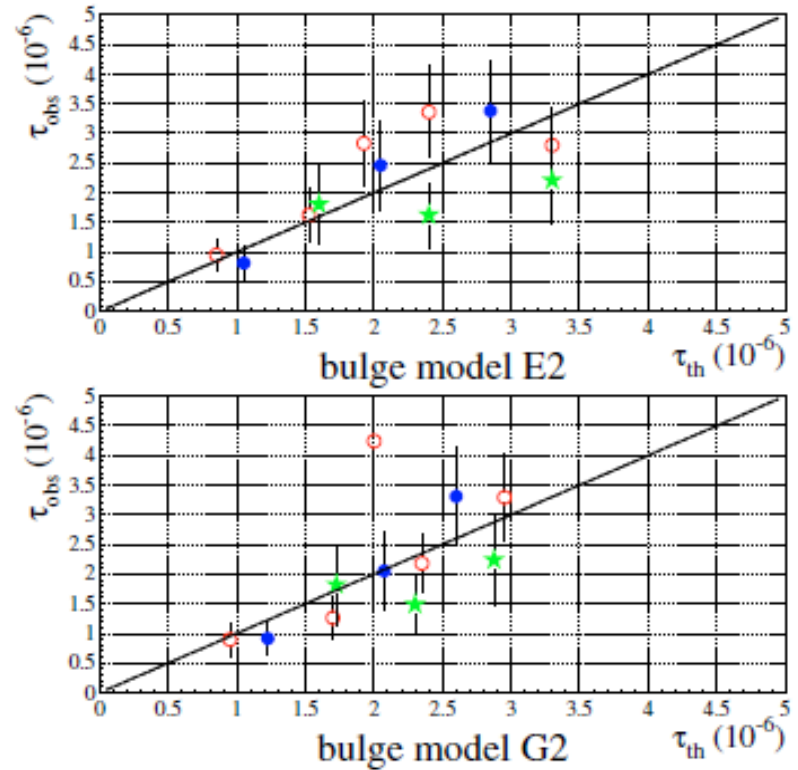


Fig. 2. The observed and the expected optical depth for the bulge models E2 (top) and G2 (see text for details). EROS, MACHO and OGLE data are the empty, filled circles and stars respectively. The solid line is the $y = x$ line.

Using microlensing and dynamical constraints of the Galaxy:

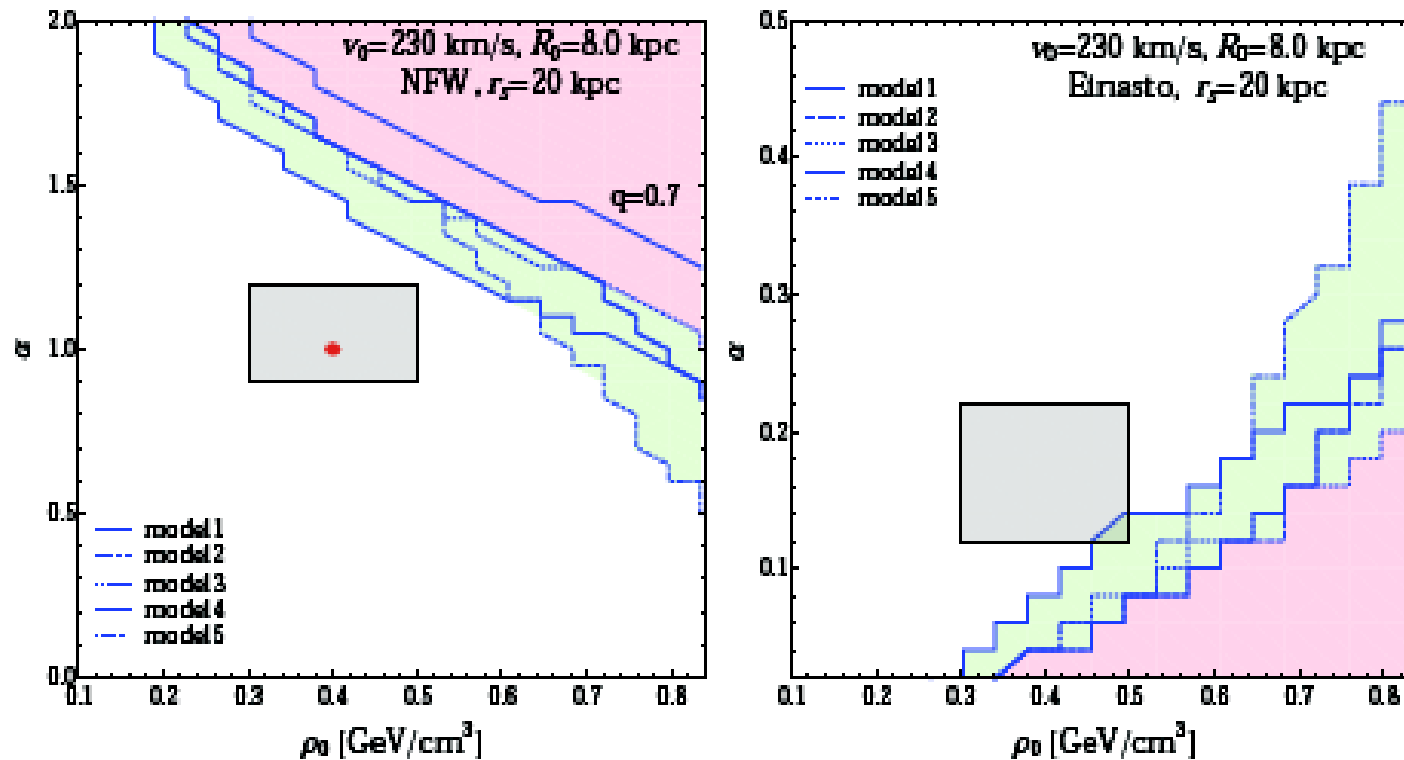
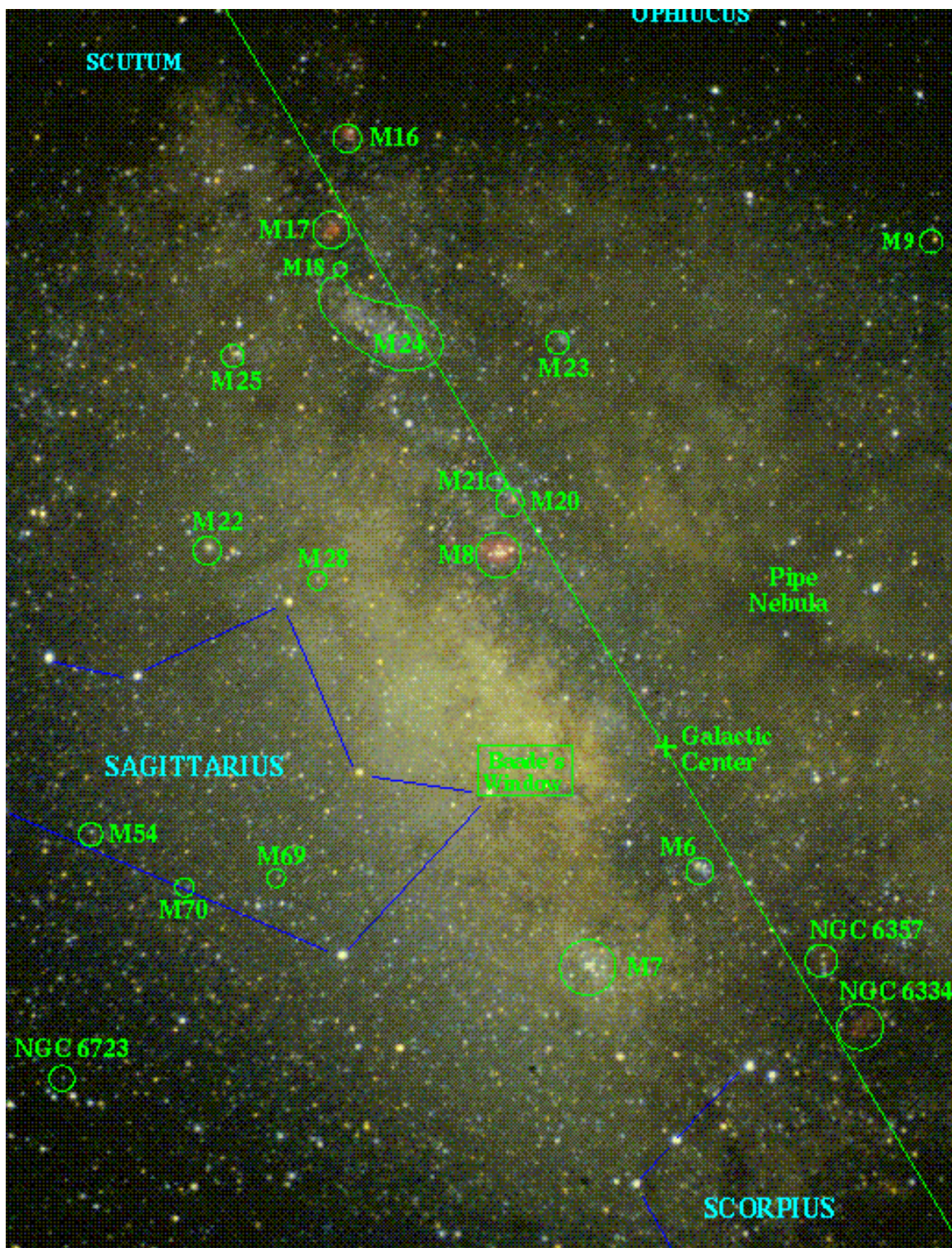
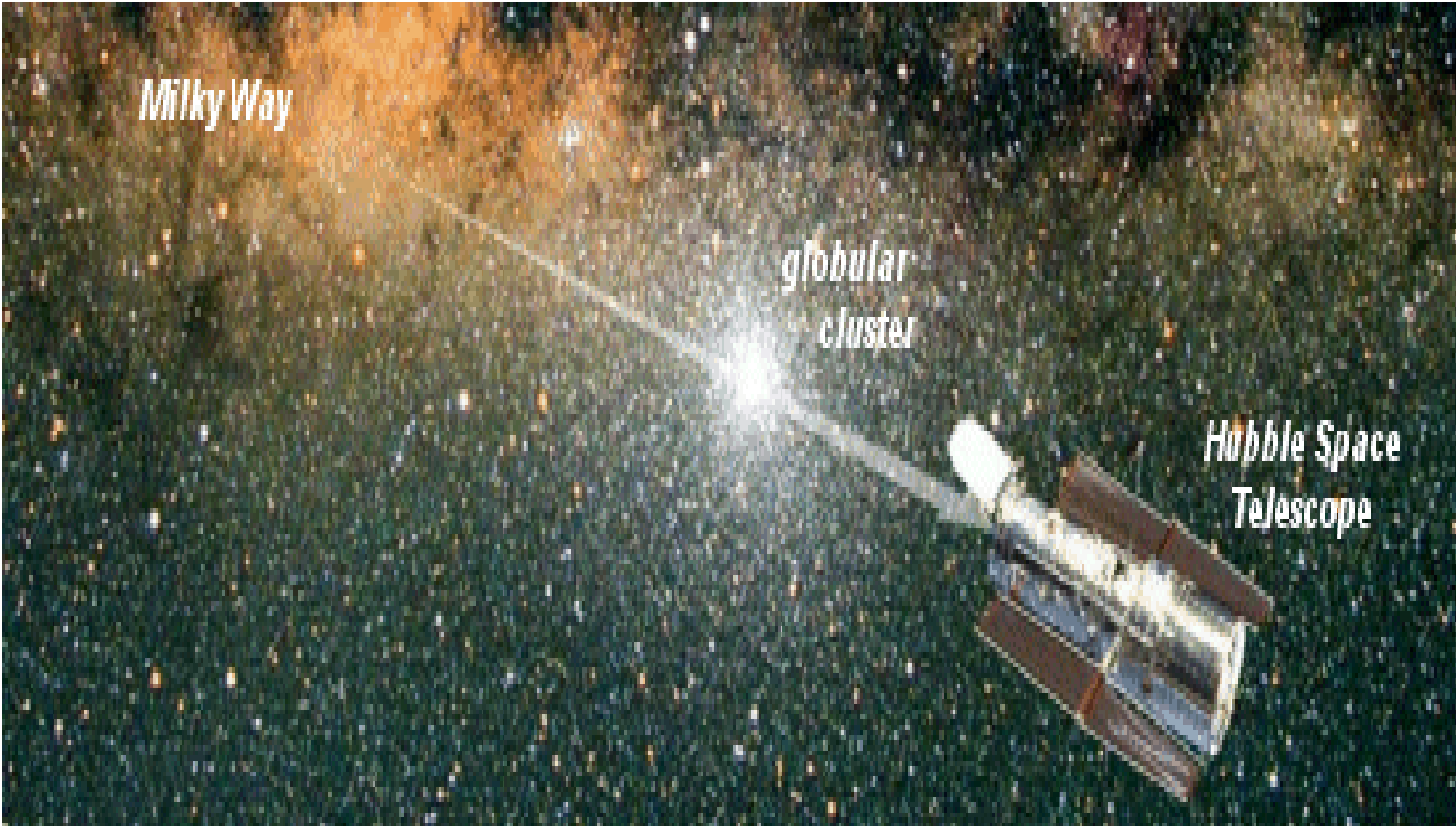
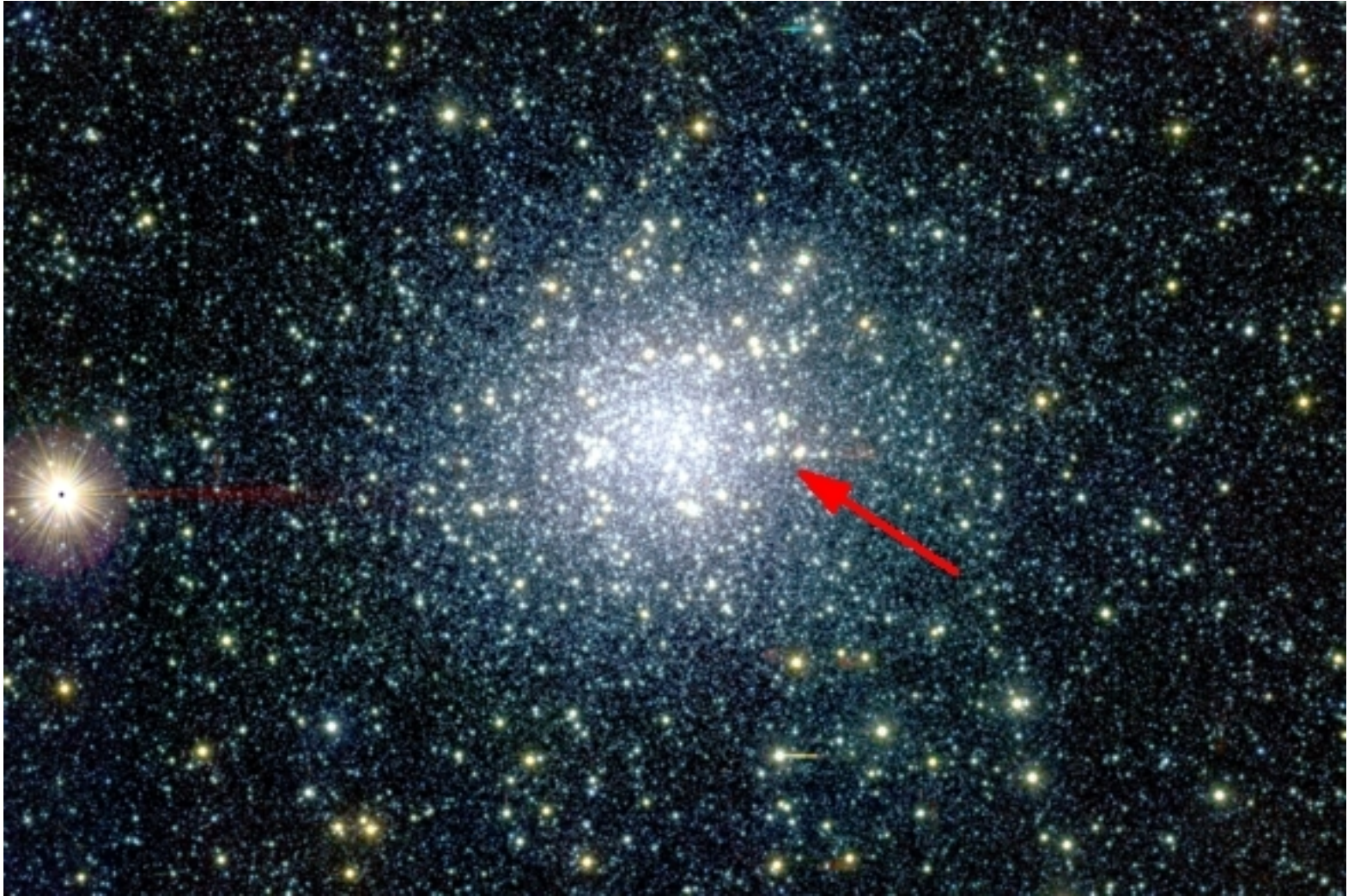


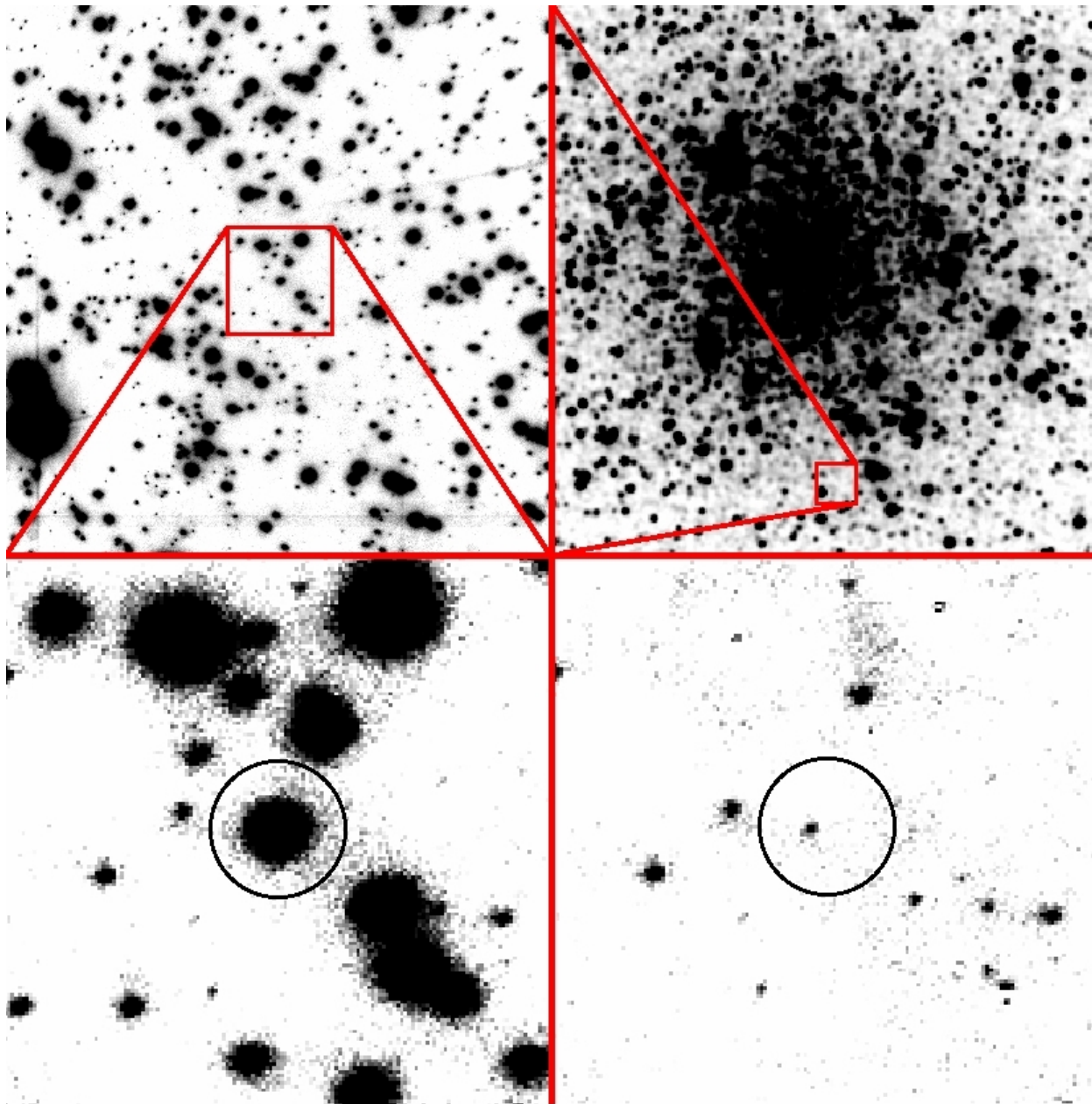
FIG. 3: Constraints on the Dark Matter distribution parameters ρ_0 and α provided by current data on the Milky Way rotation curve for a generalised NFW (left) and an Einasto (right) profile. The thick solid, thick dashed, thick dotted, thin solid and thick dot-dashed lines are the 2σ constraints in the case where the galactic baryonic component follows model 1, 2, 3, 4 and 5, respectively, all scaled to match the microlensing optical depth in equation (12). The green (light) shadowed area delimits the uncertainty on the constraint given the present-day baryonic models, while the red (dark) shadowed region indicates the excluded parameters. In the left frame, the upper thick solid line labelled “ $q = 0.7$ ” refers to the constraints for an oblate NFW profile with axis ratio $q = 0.7$ in the case of taking model 1 for the baryonic component. The shadowed rectangle encompasses the ranges of profile slopes found in numerical simulations and the values of ρ_0 found in the recent literature (see Section II), while the red filled circle in the left frame marks the parameter set ($\rho_0 = 0.4$ GeV/cm³, $\alpha = 1.0$) used to produce Figure 2. In both frames we have fixed $r_s = 20$ kpc, $R_0 = 8.0$ kpc and $v_0 = 230$ km/s.







M22 (at ~ 3 kpc distance) Arrow: position of microlensing event



M22

Mass of lens star:
 0.18 ± 0.01 solar
masses

Observed optical depth towards the Large Magellanic Cloud:

MACHO based on 13 to 17 events (~ 6 years of observations):

$$\tau = 1.0 \pm 0.3 \times 10^{-7}$$

EROS (using only bright stars) found 1 event (~ 7 years of observations):

$$\tau < 0.36 \times 10^{-7}$$

OGLE based on 2 events (~ 8 years of observations)

$$\tau = 0.16 \pm 0.12 \times 10^{-7}$$

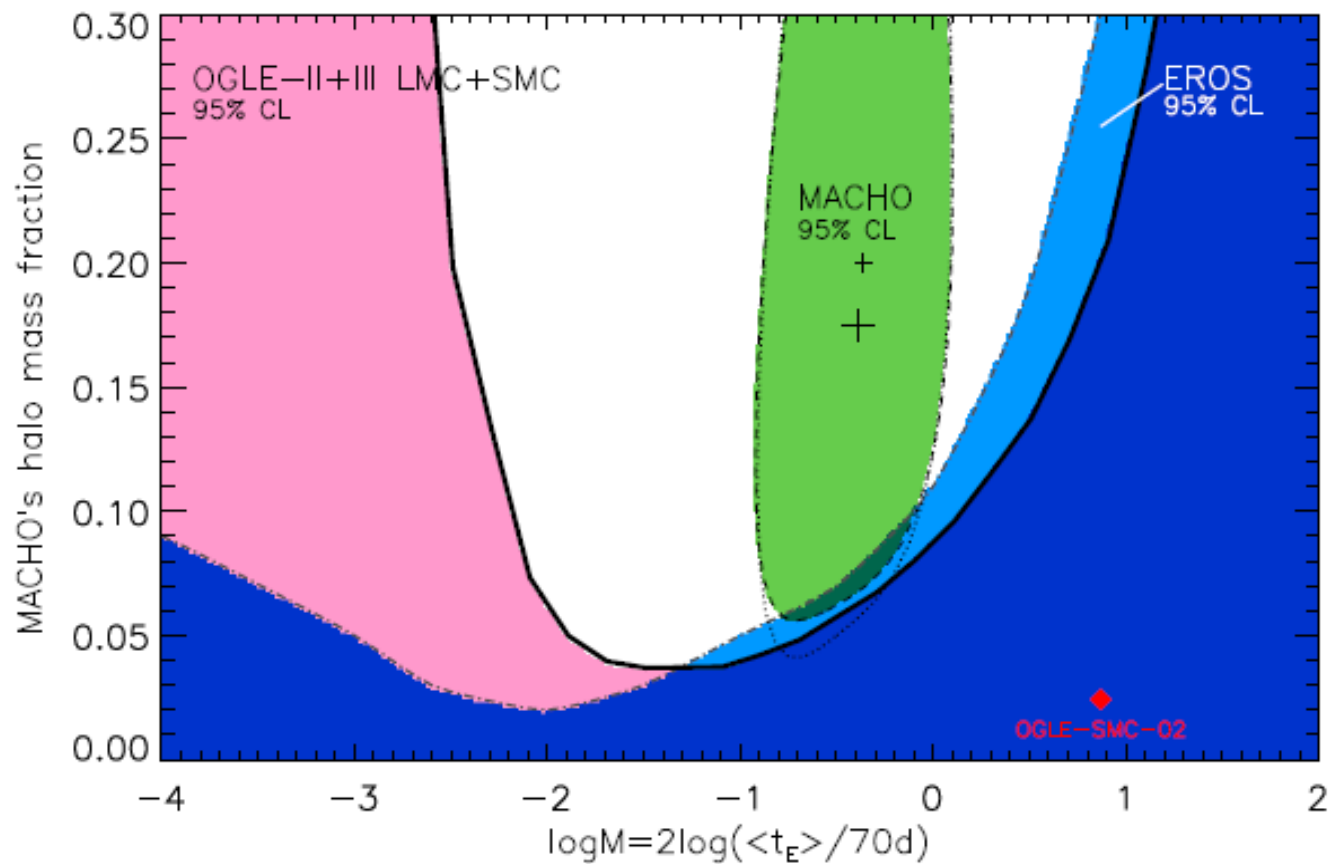


Figure 12. Inclusion region for the fraction of the mass of MACHOs in the halo for combined OGLE-II and OGLE-III data for LMC and SMC (solid curve, pink/dark blue) when all OGLE events are attributed to expected self-lensing/background signal. The EROS upper limit and the MACHO signal are shown as in Fig.11 in light/dark blue and green, respectively. Also shown is the fraction of mass due to BH-candidate event OGLE-SMC-02.

The nature and location of the observed microlensing events is still unclear.

One event by MACHO (LMC-5) and one by EROS are due to disk lenses (low mass stars).

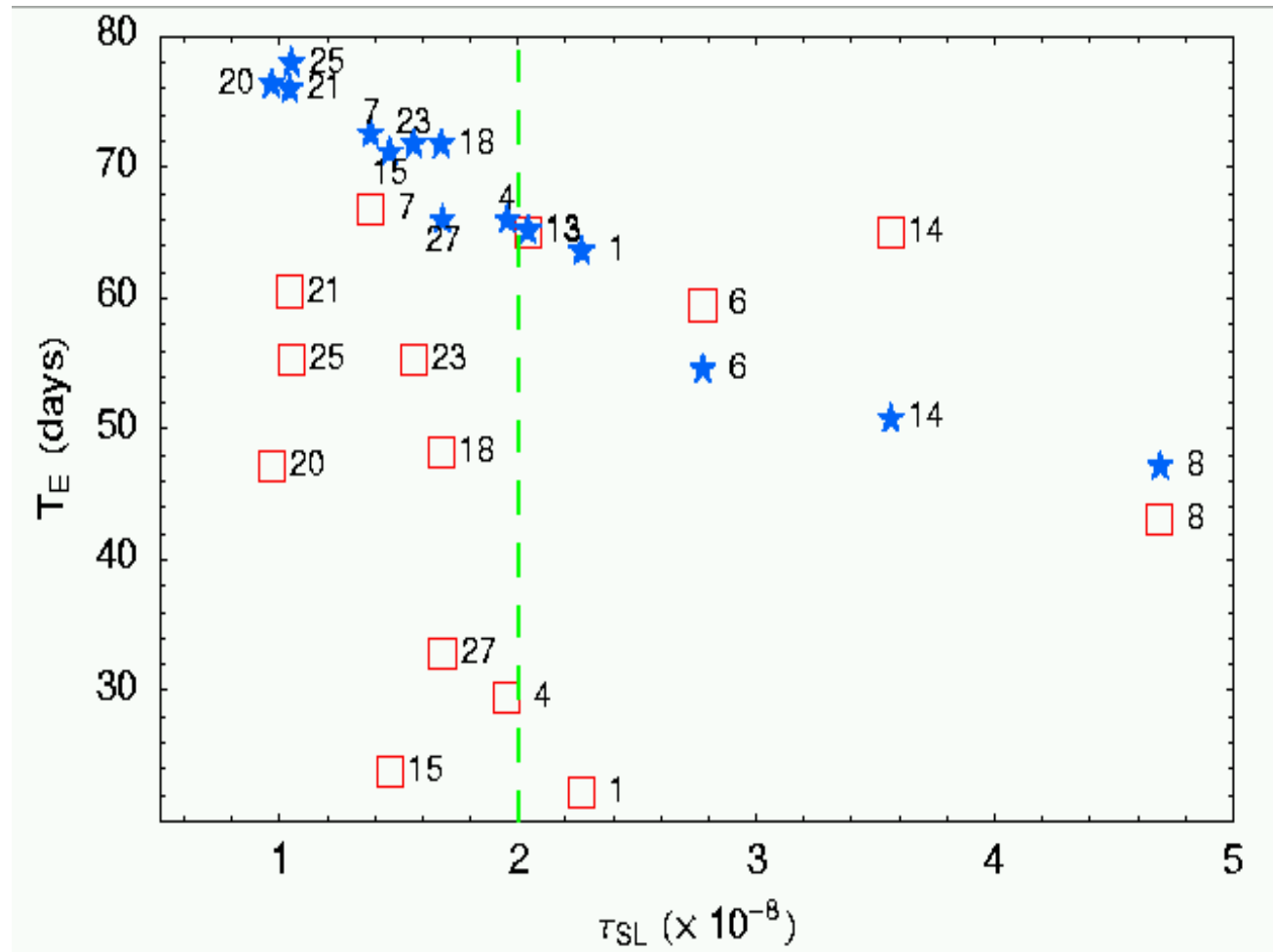
The remaining could be due to different populations:

- low mass stars in the LMC itself (self-lensing)

- MACHOs in the halo of the Milky Way

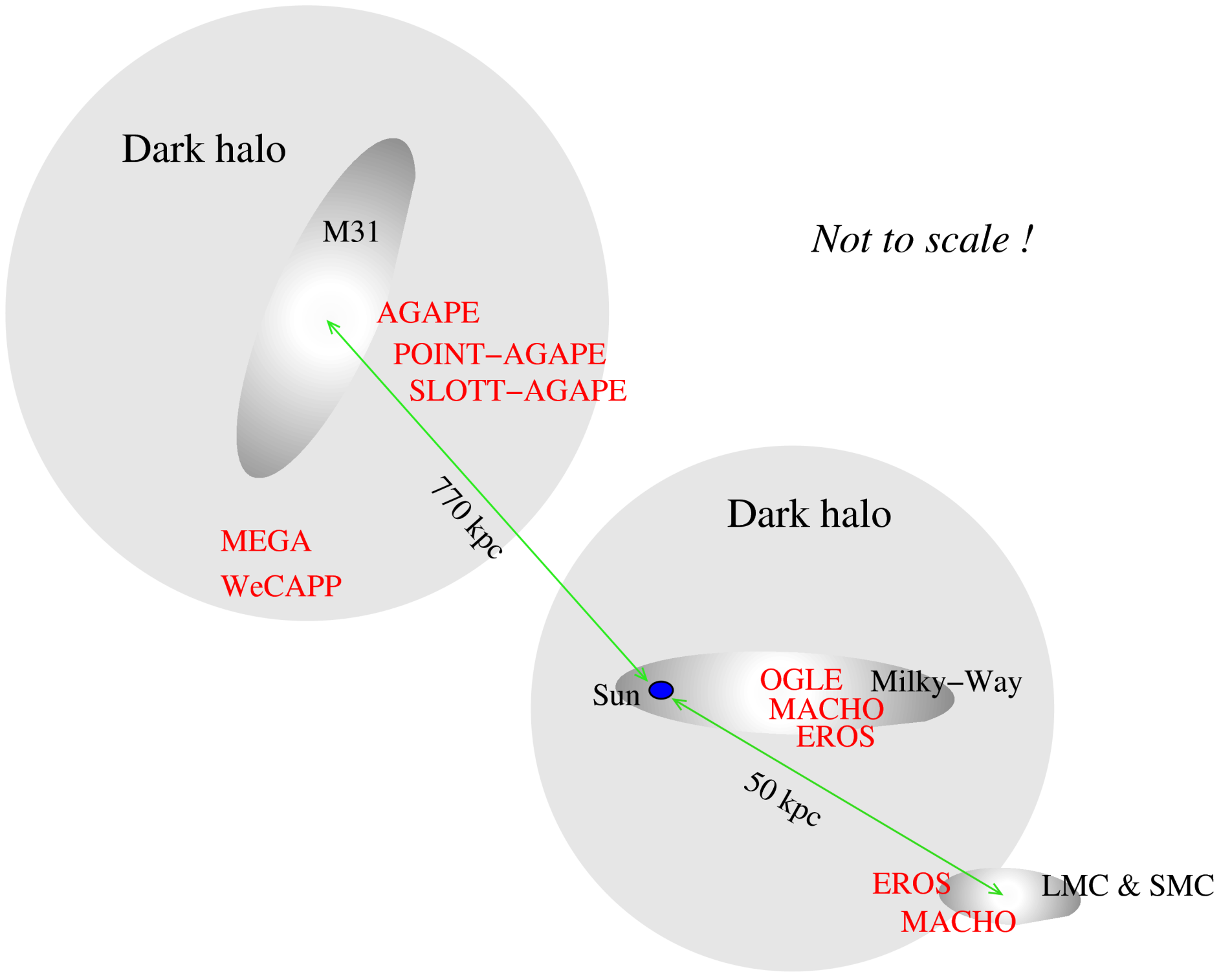
- MACHOs in the LMC halo

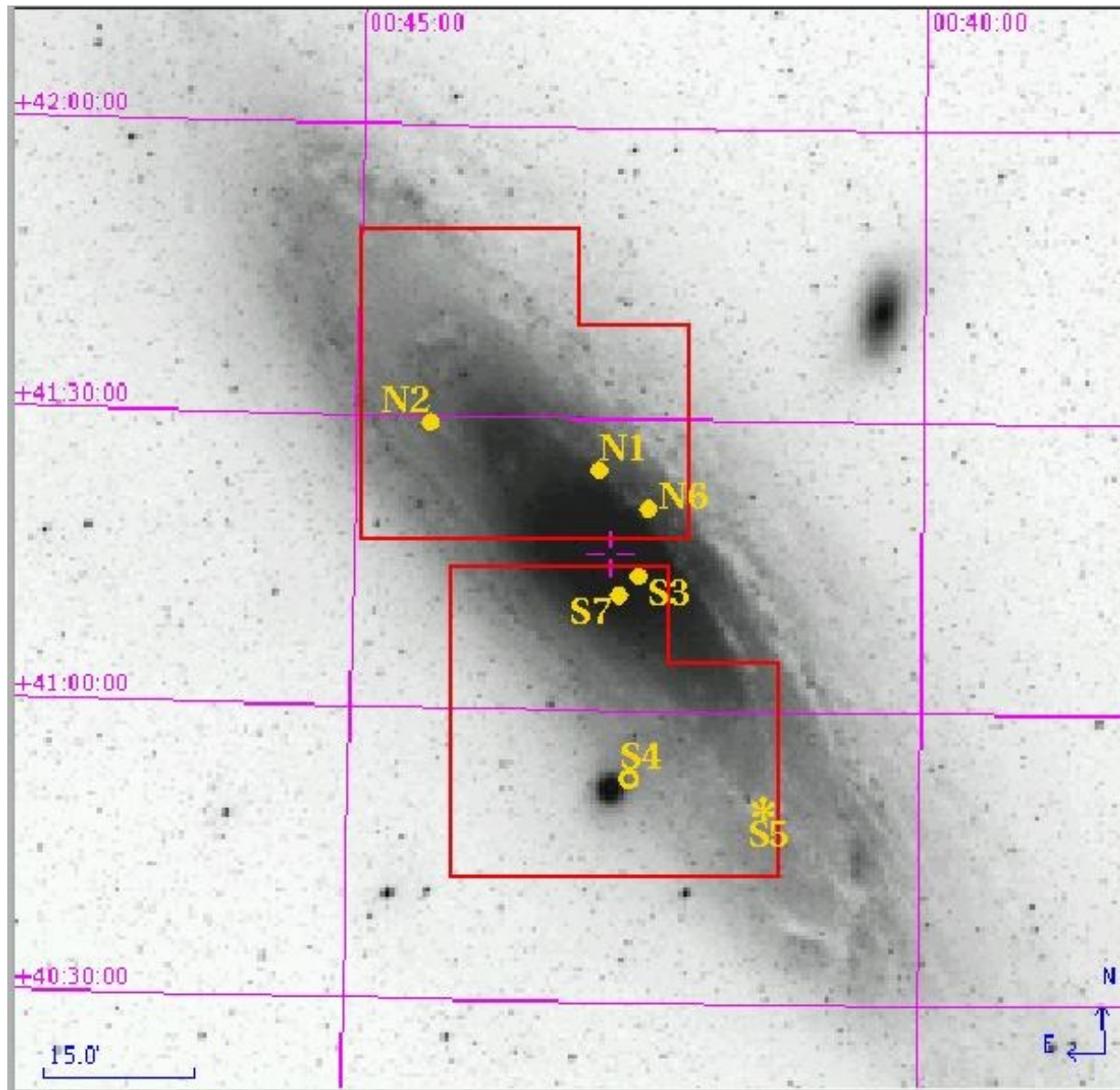
(The halo mass fraction in form of MACHOs in the LMC and Milky Way need not to be the same).



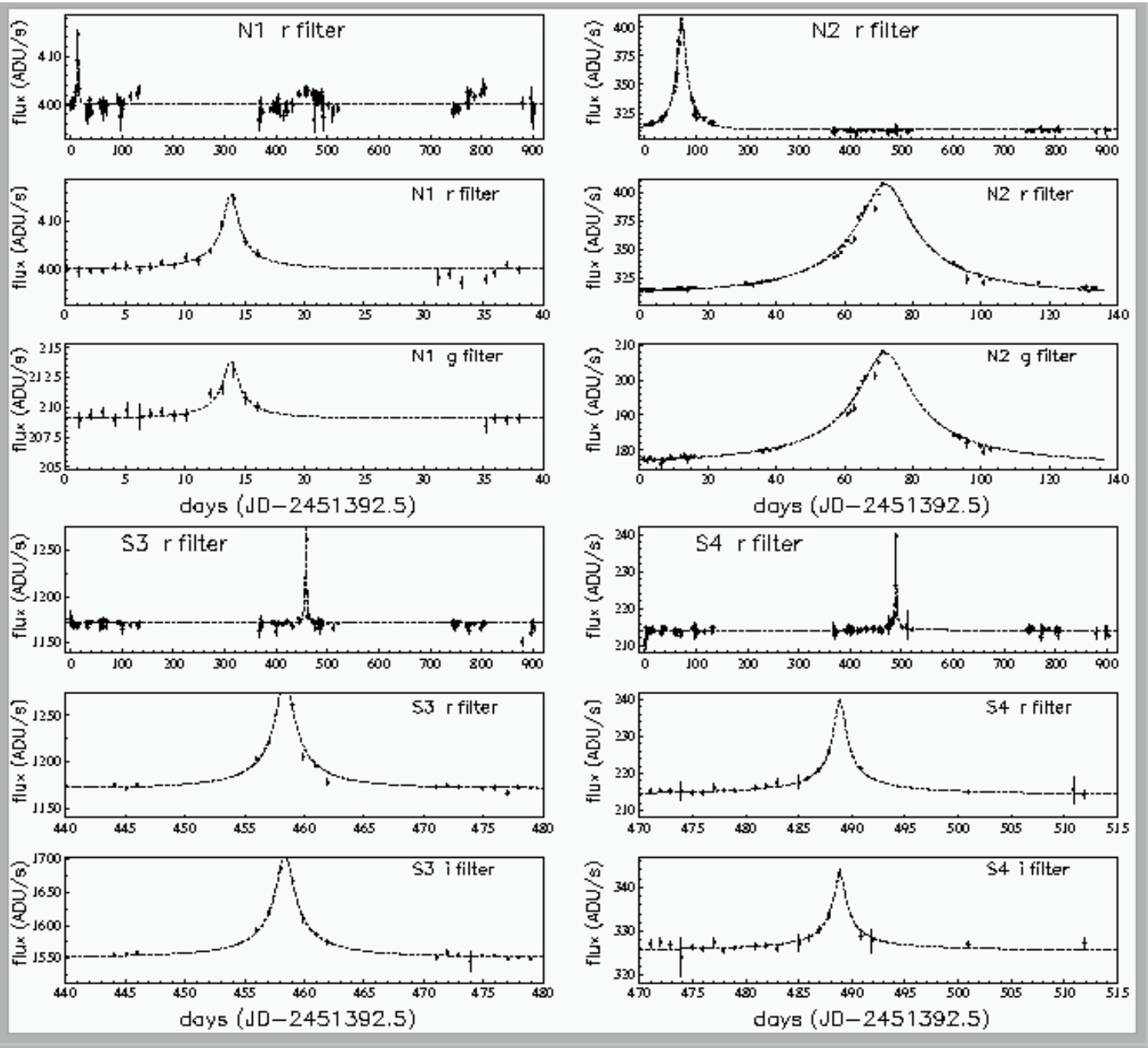
Stars: expected duration for **self-lensing** at the position where events have been observed; boxes: observed duration.

L. Mancini, PJ et al., *Astron. and Astrophys.* 427, 61 (2004)





Spatial distribution of the POINT-AGAPE microlensing candidates towards M31



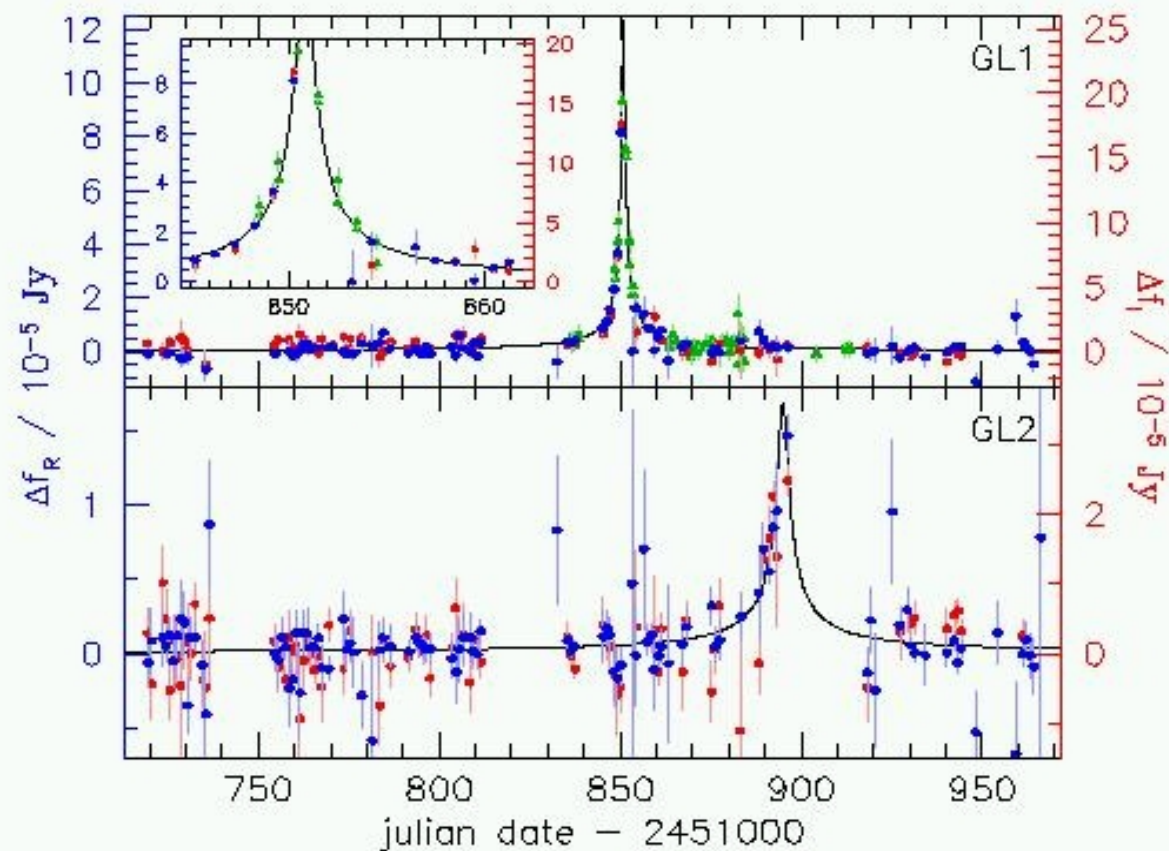
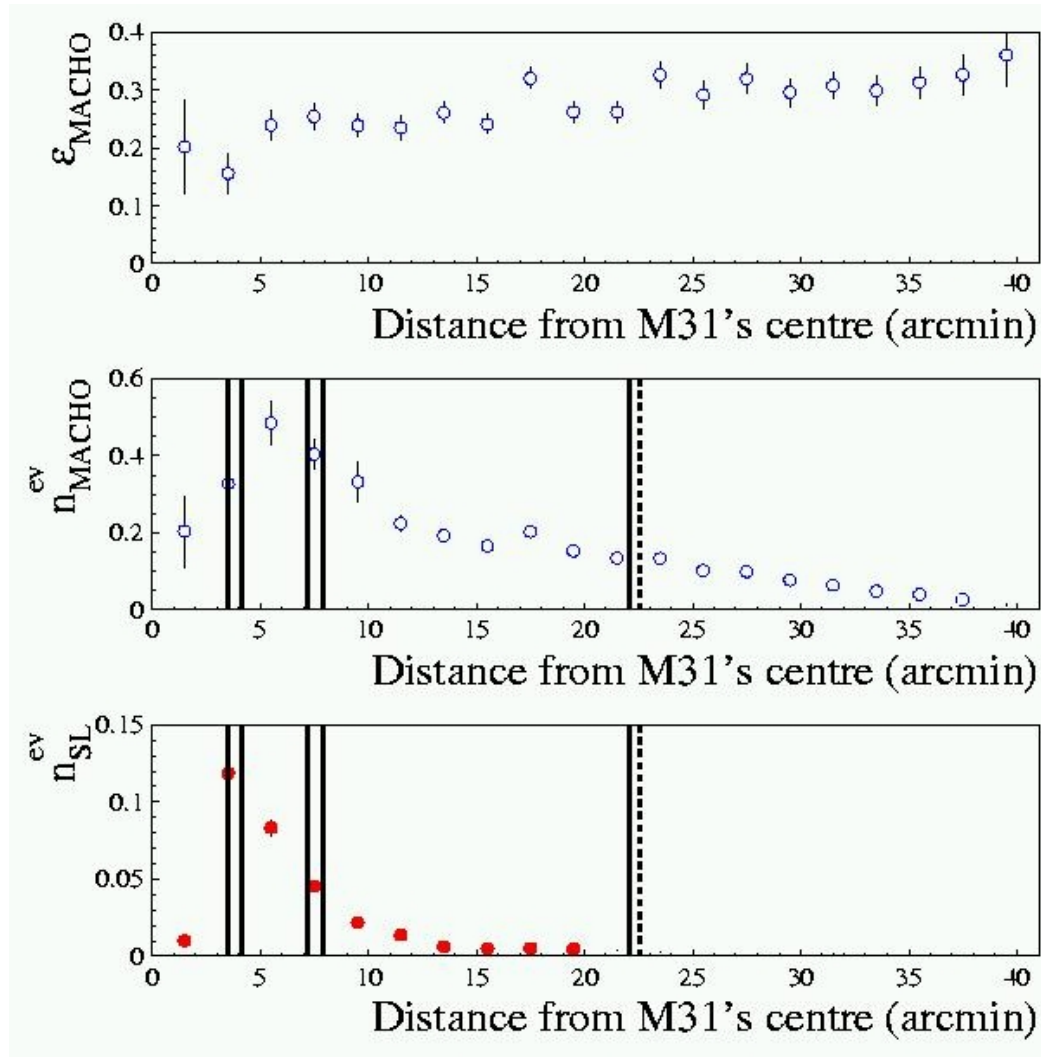
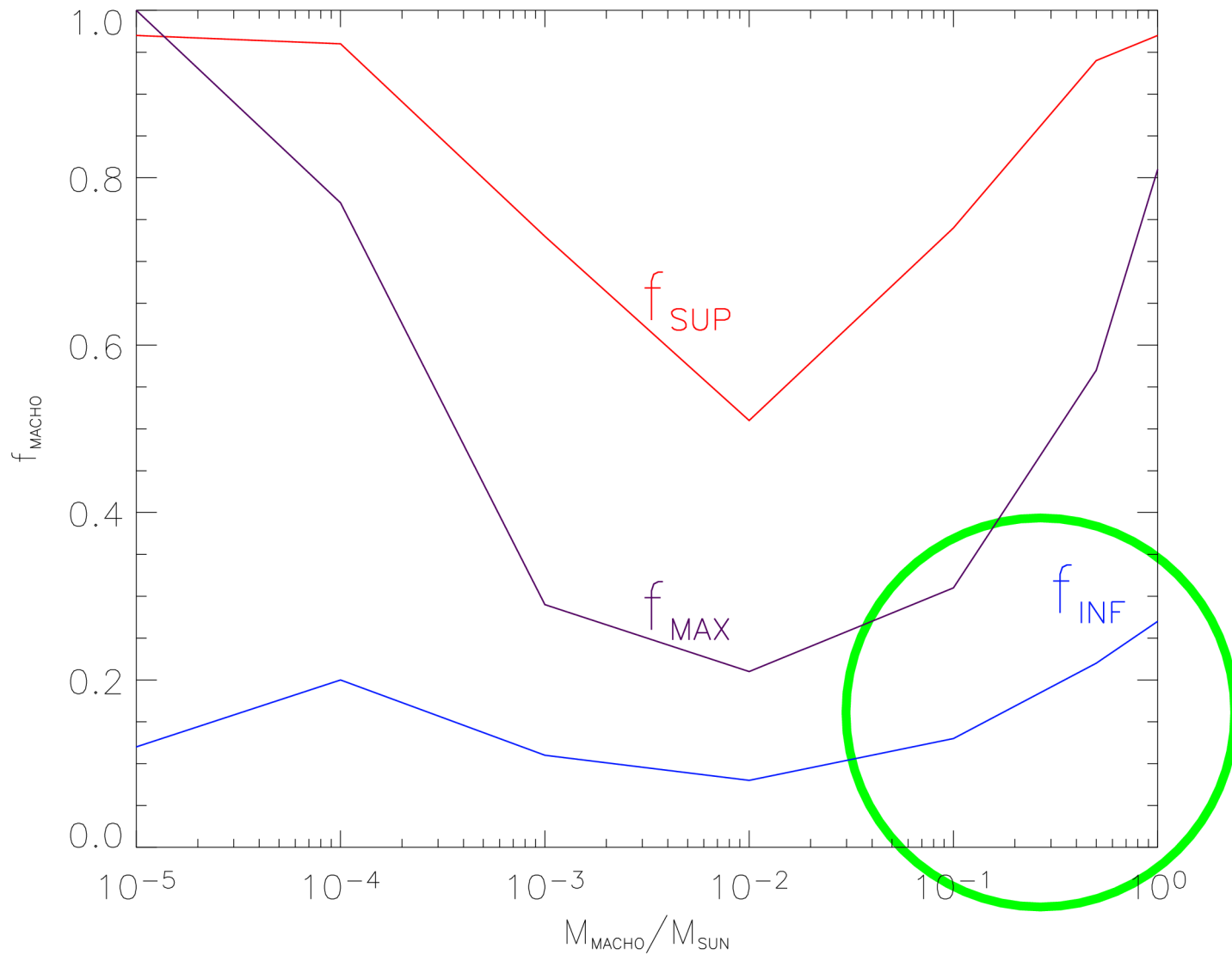


FIG. 1.— Light curves of WeCAPP-GL1 and WeCAPP-GL2. The I-band light curve (red symbols, right axis) has been scaled to the R -band light curve (blue symbols, left axis). The scaling factors were derived from the lensing fit (black curve) and correspond to a color ($R-I$) of 1.05 for GL1 and 1.08 for GL2. In addition we show the r' and i' data from the POINT-AGAPE PA-00-S3 event (green symbols) scaled to our data.

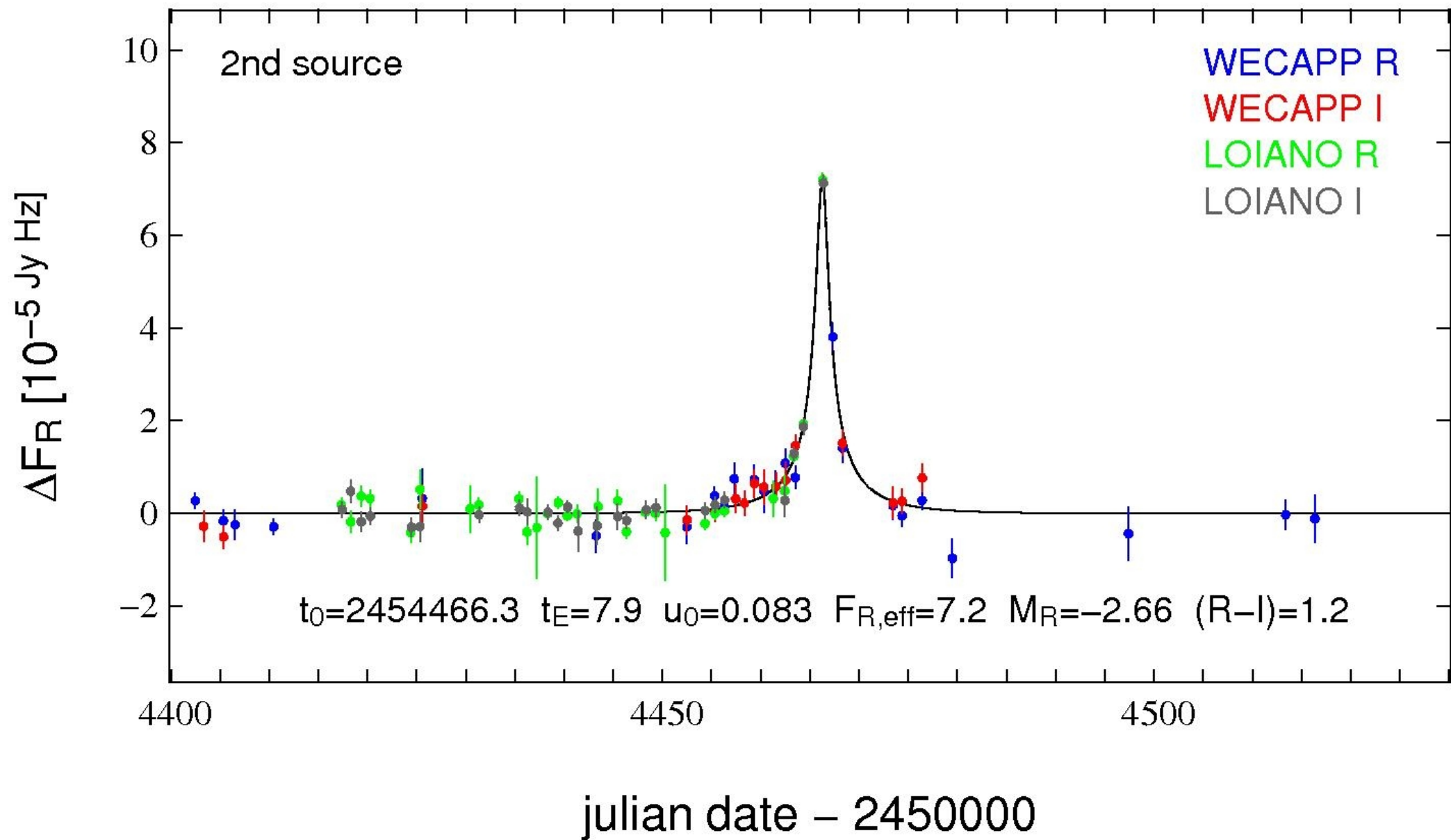


The detection efficiency and the number of predicted events as a function of the distance from the M31 center



S. Calchi Novati, PJ et al., Astron. And Astrophys. 443, 911 (2005)

Finite source size and lens proper motion:



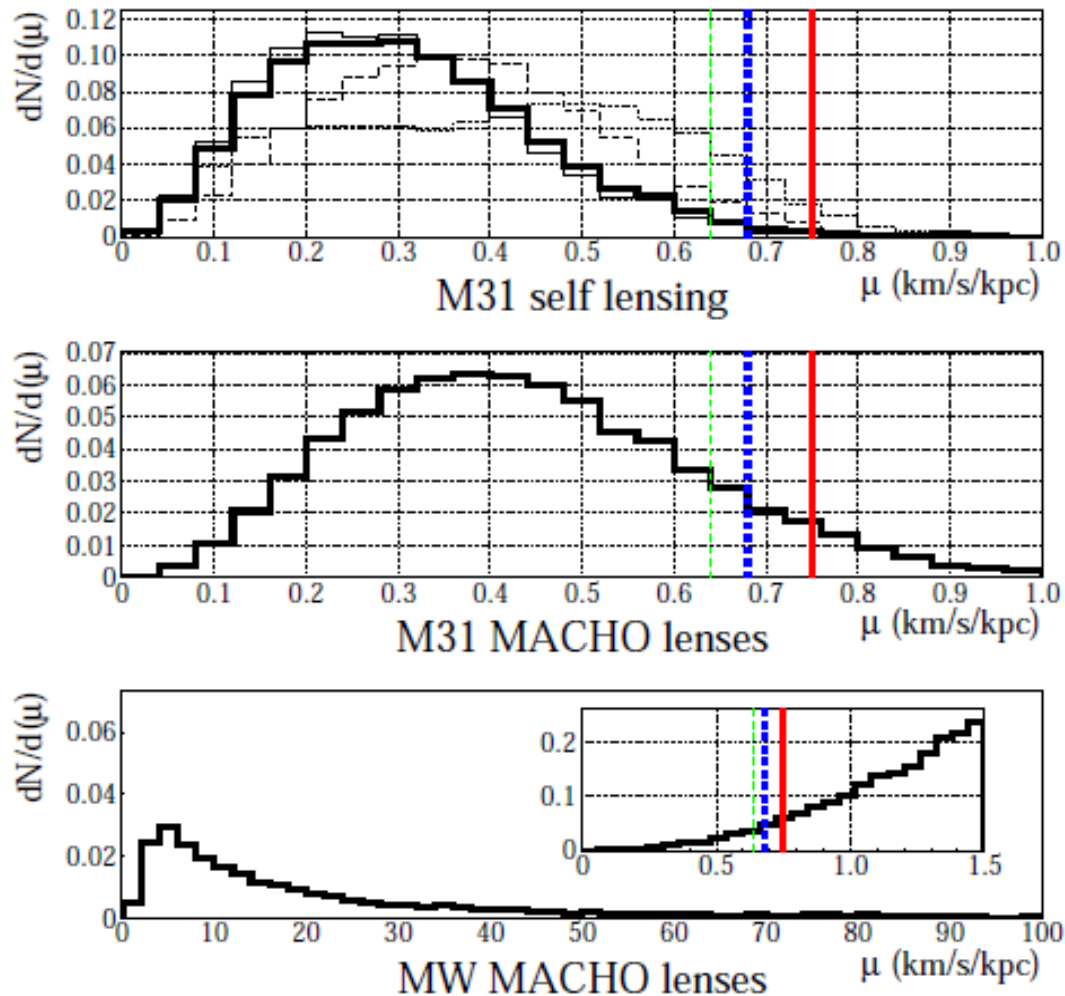
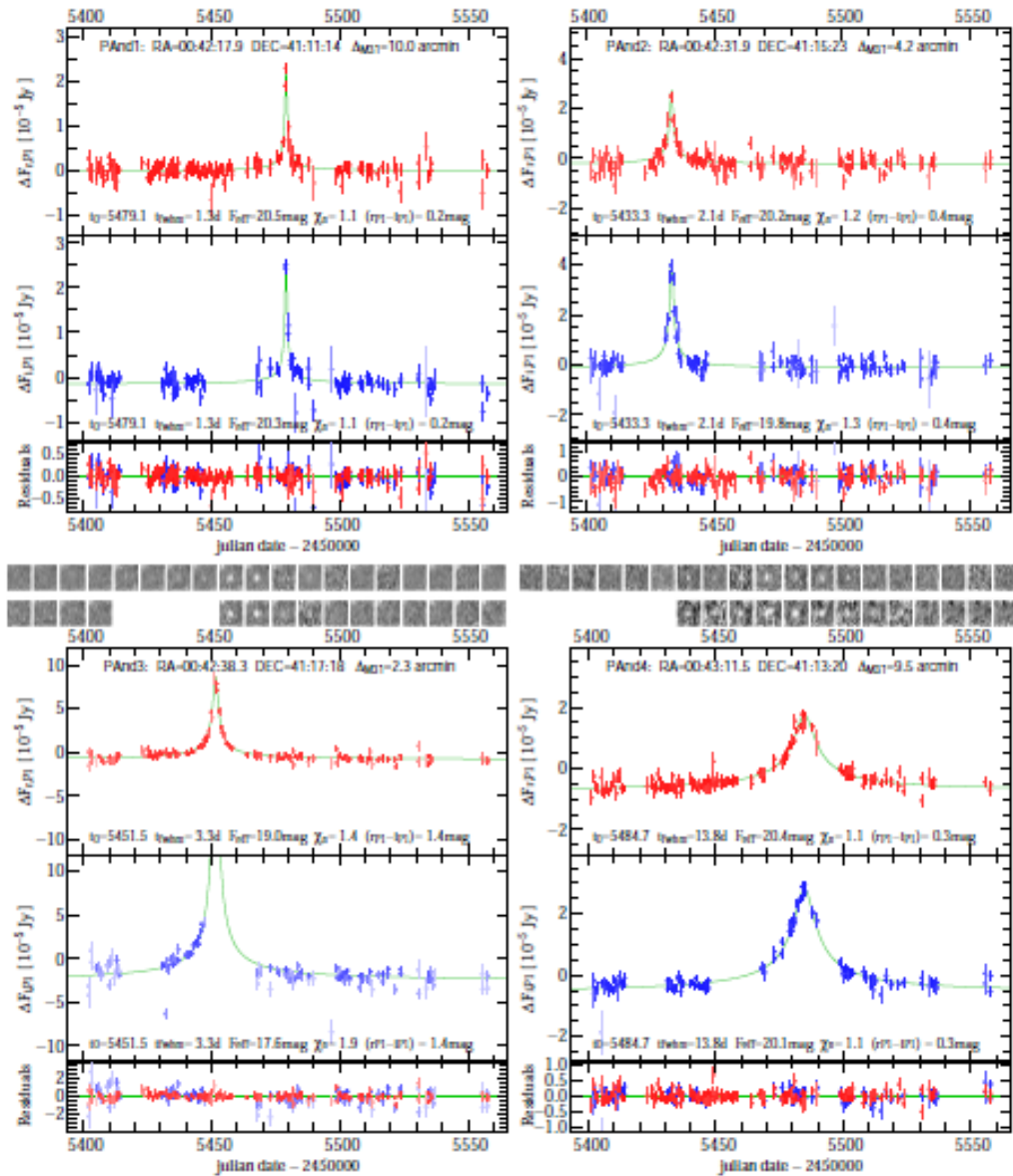
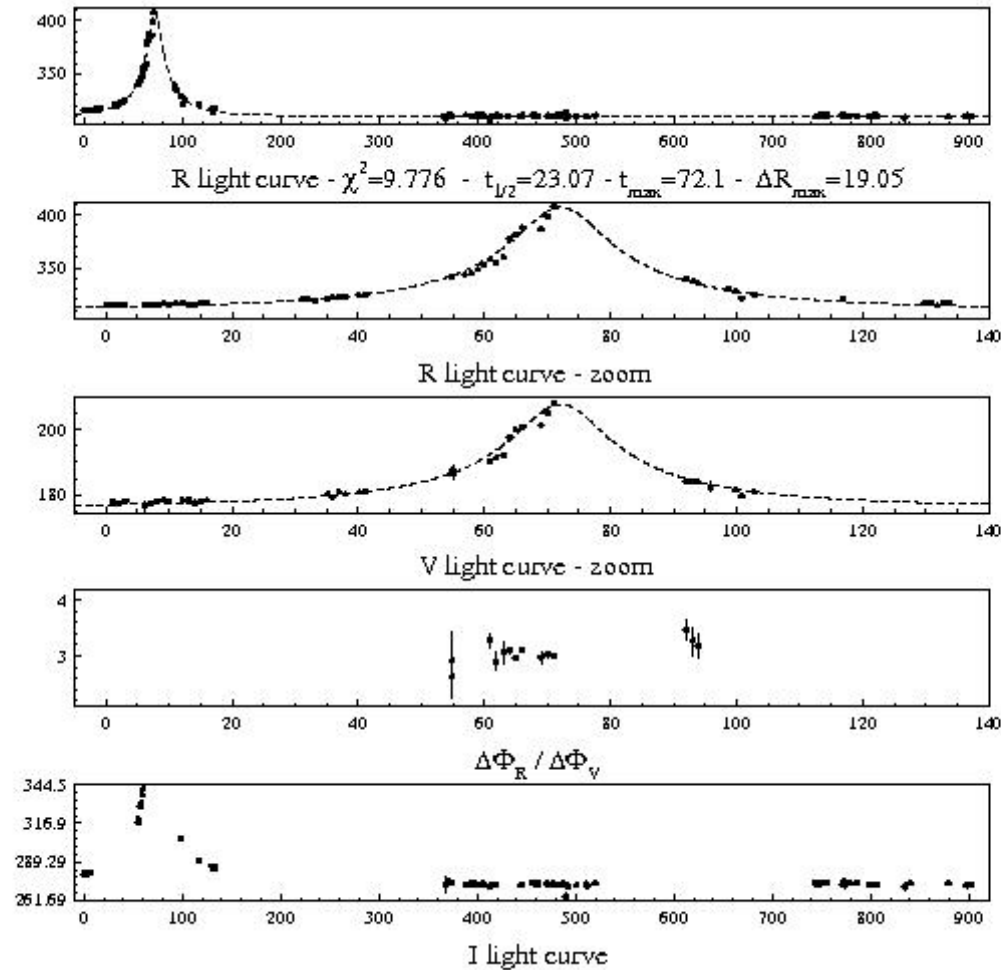


FIG. 4.— Expected distributions for the lens proper motion, μ , along the line of sight toward the OAB N2 position for different source-lens populations evaluated within the Monte Carlo simulation of the experiment. Top panel: thin solid, dashed and dotted lines are for bulge sources and bulge and disc lenses and disc-disc events, respectively; thick solid line for the overall M31 self lensing (each distribution is normalized to 1 separately). Bulge-bulge events are expected to contribute for about 80% of the expected signal; MW disc events (not shown, for which the lens proper motion distribution is expected to peak well beyond $1 \text{ km s}^{-1} \text{ kpc}^{-1}$) are expected to be negligible (see text for details). Middle (bottom) panels: M31 (MW) MACHO lenses with the overall (M31+MW) MACHO distributions normalized to 1, and 75% signal expected from M31 lenses (in the inset, bottom panel, showing a zoom for the MW MACHO distribution, the units are 10^{-3}). The solid, dashed and thin dashed vertical lines (68.3%, 90% and 95% level, respectively) indicate the *lower* limit for the lens proper motion derived in the light curve analysis (Sect. 2.2, Fig. 3).



C.H.Lee et al, *Astronomical J.*, 143, 89 (2012) (Pan-STARRS survey)



G. Ingresso, PJ et al., MNRAS 399, 219 (2009) (Pixel-lensing a way to detect extrasolar planets in M31)

Outlook:

- Microlensing is an important tool to study the structure of our galaxy and thus of its dark matter content
- Some of the events are due to LMC **self-lensing** and other Components (galactic disk). The contribution of a small ($\sim 5-10\%$?) component is still possible
- Microlensing events towards M31 have been successfully found (self-lensing?). Their contribution to the halo is still an open issue
- Microlensing is now a mature and established tool, which is useful also for finding planets (both in our Galaxy but also in M31 !)
- Need more observations!